

Modern Valence-Bond-Like Representations of Selected D_{6h} “Aromatic” RingsJ. Grant Hill,[†] David L. Cooper,^{*,‡} and Peter B. Karadakov^{*,†}*Department of Chemistry, University of York, Heslington, York YO10 5DD, U.K., and Department of Chemistry, University of Liverpool, Liverpool L69 7ZD, U.K.**Received: December 22, 2005; In Final Form: May 4, 2006*

Starting from CASSCF(6,6)/6-31G(d,p) wave functions, we consider different valence-bond (VB)-like interpretations of the π electron systems for various (constrained) “benzene-like” D_{6h} rings, exploiting the invariance of the total wave function to arbitrary nonsingular transformations of the active orbitals. Quantities obtained rather directly from the various calculations provide a fairly consistent ordering of the degree of aromaticity: $C_6H_6 \sim B_6 > N_6 > Al_6 \sim Si_6H_6 > P_6$. Representations based on mutually orthogonal orbitals are found to be somewhat less satisfactory than those that have no such constraints on the overlaps between the active orbitals.

Introduction

As is well-known, aromaticity is one of a number of remarkably important but “fuzzy” concepts in chemistry that does not lend itself easily to widely applicable clear-cut definitions.¹ Theoretical studies tend to emphasize the particular bonding patterns of the π electrons, even though the σ framework must also play a key role in determining the preference for particular features of the optimal geometries.² The present work was prompted by a comparative study using the CiLC method³ of the description of the π electron systems in the (constrained) “benzene-like” D_{6h} ring systems in C_6H_6 , Si_6H_6 , B_6 , Al_6 , N_6 and P_6 . A link was suggested between the degree of aromaticity in these six molecules and the differences between the weights of certain “minority” valence-bond-like components in CASSCF wave functions. Unlike those that one normally envisages in traditional valence-bond (VB) descriptions, the localized orbitals in the CiLC method are orthogonal, and so we were very interested to compare analogous descriptions that are based instead on nonorthogonal orbitals associated with valence-bond-like components that dominate the corresponding CASSCF wave functions.

Computational Procedure

Geometries were optimized for the six ring systems at the CASSCF(6,6)/6-31G(d,p) level within the constraint of D_{6h} symmetry, whether or not this leads to the most stable structure. Our aim, as in the previous work,³ was to compare the descriptions of the π bonding for the (constrained) “benzene-like” geometries. Frequency calculations show the optimized geometries for C_6H_6 ($r_{CC} = 1.3961$ Å, $r_{CH} = 1.0759$ Å) and P_6 ($r_{PP} = 2.1213$ Å) to be true minima at this level of theory, but N_6 ($r_{NN} = 1.3014$ Å) has a sole imaginary frequency: the form of the corresponding normal mode suggests that this molecule would remain planar at a lower-energy geometry but would no longer have equal N–N bond lengths. Al_6 ($r_{AlAl} = 2.4586$ Å) also has one imaginary frequency, whereas both B_6 ($r_{BB} =$

1.5997 Å) and Si_6H_6 ($r_{SiSi} = 2.2292$ Å, $r_{SiH} = 1.4697$ Å) possess three imaginary frequencies, and analysis of the corresponding normal modes shows that nonplanar geometries would be more stable in these cases. All of these calculations were initially carried out using the GAUSSIAN98 package⁴ but the optimizations were subsequently repeated using MOLPRO⁵ (yielding, of course, the same results). All of the calculations used the 6-31G(d,p) basis set in Cartesian form (six d components).

These CASSCF(6,6)/6-31G(d,p) wave functions are of course invariant to arbitrary nonsingular linear transformations of the six active molecular orbitals. In the CiLC approach,³ the active orbitals are localized by means of a unitary transformation that preserves orthogonality. The weights in the CASSCF wave function of configurations built from these localized orbitals are then determined by a subsequent CI calculation, with, of course, the same configuration list as in the CASSCF. The outcome is an alternative representation of the original CASSCF wave function.

The alternative, arguably more rigorous strategy that we employ here is to perform a general transformation of the orbitals that, in some sense, maximizes the importance in the CASSCF wave function Ψ_{CAS} of a valence-bond-like component Ψ_{VB} . For this last, we chose here to use a spin-coupled-like wave function:⁶

$$\Psi_{VB} = \hat{A} \left[\left(\prod_{i=1}^n \phi_i \alpha \phi_i \beta \right) \left(\prod_{\mu=1}^6 \psi_{\mu} \right) \Theta_{00}^6 \right] \quad (1)$$

in which the ϕ_i are inactive orbitals (taken directly from the converged CASSCF calculation), the ψ_{μ} are the six singly occupied active orbitals (determined as linear combinations of the CASSCF active orbitals), and Θ_{00}^6 is the optimal active-space spin function for $N = 6$ electrons with spin quantum numbers $S = M_S = 0$. The calculations described here were performed with the CASVB module⁷ in MOLPRO,⁵ which provides different criteria for choosing the “optimal” transformation of the active orbitals. One such approach involves maximizing the overlap between Ψ_{CAS} and Ψ_{VB} . Specifically, one maximizes

* Corresponding authors. E-mail addresses: D.L.C., dlc@liverpool.ac.uk; P.B.K., pbk1@york.ac.uk.

[†] University of York.

[‡] University of Liverpool.

$$S_{\text{VB}} = \frac{\langle \Psi_{\text{CAS}} | \Psi_{\text{VB}} \rangle}{\langle \Psi_{\text{VB}} | \Psi_{\text{VB}} \rangle^{1/2}} \quad (2)$$

Another standard approach involves minimizing the energy E_{VB} of the VB-like component:

$$E_{\text{VB}} = \frac{\langle \Psi_{\text{VB}} | \hat{H} | \Psi_{\text{VB}} \rangle}{\langle \Psi_{\text{VB}} | \Psi_{\text{VB}} \rangle} \quad (3)$$

Whichever criterion is chosen, all of the CI coefficients in the full CASSCF wave function are transformed simultaneously with the orbitals, so that one of the outcomes is an alternative representation of the original CASSCF wave function.

As well as the form of Ψ_{VB} , it proves useful to examine its orthogonal complement Ψ_{VB}^{\perp} within Ψ_{CAS} , defined according to

$$\Psi_{\text{CAS}} = S_{\text{VB}} \Psi_{\text{VB}} + (1 - S_{\text{VB}}^2)^{1/2} \Psi_{\text{VB}}^{\perp} \quad (4)$$

We denote by W_i the accumulated total Chirgwin–Coulson⁸ weight in Ψ_{VB}^{\perp} of VB-like structures with I doubly occupied orbitals and we define an effective total weight W_{VB} for Ψ_{VB} by requiring that $W_{\text{VB}} + W_1 + W_2 + W_3$ is unity (or 100%).

An important additional feature of the CASVB module in MOLPRO is the ability to perform also fully variational calculations. This allowed us to calculate fully optimized modern VB wave functions of the form of eq 1, optimizing all of the ϕ_i and ψ_{μ} , as well as the active-space spin function Θ_{00}^6 . The results matched those obtained using our own standalone spin-coupled codes.⁹ We denote the resulting spin-coupled wave functions Ψ_{SC} .

Within MOLPRO, extracting spin-coupled-like wave functions from CASSCF is several times cheaper than the analogous fully variational SC calculation, but the CPU time required for the latter is still rather modest, typically being less than for the corresponding CASSCF calculation which precedes it.

In all, we performed three types of calculation at the optimized D_{6h} geometries listed earlier:

A. Transformation of the CASSCF wave function to an alternative modern-VB-dominated representation, using the E_{VB} energy-based criterion (see eq 3), without any constraints on the overlaps between the active orbitals ψ_{μ} .

B. The same as in A, except that all of the active orbitals ψ_{μ} are constrained to be mutually orthogonal.

C. Fully variational determination of spin-coupled wave functions. We imposed σ – π separation, so as to enable proper comparisons with A and B.

Results and Discussion

As explained in the previous section, we examined two different transformations of the CASSCF active space orbitals that maximize the importance within the total wave function of a VB-like component Ψ_{VB} of the form shown in eq 1. The total CASSCF wave function Ψ_{CAS} and energy E_{CAS} are of course invariant to such a change of representation. The two different transformations considered here are both based on minimizing E_{VB} (eq 3) but, in one case, we constrained the active orbitals ψ_{μ} to remain mutually orthogonal. We start by examining the optimal representation that has no such constraints, so that all of the ψ_{μ} are allowed to overlap with one another.

Given that it is directly optimized, the proximity of E_{VB} to E_{CAS} is an important measure of the extent to which Ψ_{VB} dominates Ψ_{CAS} . From the energies listed in Table 1, we see that the differences are 7–8 mhartrees for the rings based on

first-row atoms and 4–5 mhartrees for those based on second-row atoms. Further indications that Ψ_{VB} dominates Ψ_{CAS} are provided by the values of S_{VB} (eq 2) and the various Chirgwin–Coulson weights that are listed in Table 1. The accumulated total Chirgwin–Coulson weights W_i in the orthogonal complement Ψ_{VB}^{\perp} (eq 4) of structures with I doubly occupied orbitals are all rather small, and so the effective total weights W_{VB} for Ψ_{VB} in Ψ_{CAS} are all on the order of 99%. The largest contributions to Ψ_{VB}^{\perp} come from structures with two doubly occupied orbitals, such that W_2 reaches 1% in Al_6 . Values of W_1 are somewhat smaller and those of W_3 are almost vanishingly small. The values of S_{VB} , which measure the degree of overlap between Ψ_{VB} and Ψ_{CAS} , lie in the range 0.993–0.996 for these ring systems. Slightly higher values could no doubt be achieved by optimizing S_{VB} , but the differences from unity are already rather small.

This dominance of Ψ_{VB} in Ψ_{CAS} makes it very worthwhile to examine in some detail the optimal form of Ψ_{VB} . For each ring system, we obtained a solution with six symmetry equivalent, relatively localized nonorthogonal active orbitals ψ_{μ} . These orbitals are shown in the left-hand column of Figure 1 by means of contours, drawn in a consistent fashion, for the plane 0.5 Å above the molecular plane. The contour heights selected for a given ψ_{μ} depend only on the maximum value of $|\psi_{\mu}|$ in the chosen plane, according to $\pm(i/9) \max |\psi_{\mu}|$ for $i = 1, 2, \dots, 9$. Unbroken contours correspond to positive values and broken contours (if any) to the analogous negative values. The same orbitals are also depicted in the left-hand column of Figure 2, which was generated by selecting isovalues $\pm v$ with v scaling with respect to the $v = 0.085$ value selected for benzene as $v = 0.085 \max |\psi_{\mu}| / \max |\psi_{\mu}(\text{C}_6\text{H}_6)|$ where the $\max |\psi_{\mu}|$ values are those used to select the contour heights in Figure 1. The remaining active orbitals for each ring system can of course be obtained from these by symmetry operations of the D_{6h} point group. The ψ_{μ} are clearly based on p_{π} functions that are deformed mostly toward neighboring atoms, thereby enhancing the nearest-neighbor orbital overlaps (which are listed in Table 1). All of the remaining orbital overlaps are somewhat smaller. A further consequence of the orbital deformations is the low value of W_1 in each system.

Further insights into the form of Ψ_{VB} are provided by examining the composition of the active-space spin function (Θ_{00}^6 in eq 1). As is well-known, there are five linearly independent modes of coupling the spins of six electrons so as to achieve an overall singlet. For systems of the type considered here, it is probably most natural to examine the Chirgwin–Coulson weights of these different modes in the traditional Rumer basis. Rumer functions 1 and 4 are the familiar Kekulé-like modes, so that functions 2, 3, and 5 are the para-bonded or Dewar-like modes. The Chirgwin–Coulson weights P_K of a single Kekulé-like mode of spin coupling are all of the order of 38–40% (see Table 1), consistent with fairly traditional VB notions of aromaticity.

We turn now to analogous representations of the same CASSCF wave functions, again minimizing E_{VB} , but now insisting also on mutual orthogonality of all six active orbitals. As before, we obtained solutions with six symmetry equivalent, relatively localized ψ_{μ} . The shapes of these orbitals are shown in the right-hand columns of Figures 1 and 2. A key difference from those obtained without such orthogonality constraints is a reduction in the degree of deformation toward neighboring atoms, except that there are now small orthogonalization tails on the adjacent centers. There is also a dramatic reduction in the Chirgwin–Coulson weights P_K of a single Kekulé-like mode

TABLE 1: Key Quantities Obtained by Optimizing the Importance of Ψ_{VB} in Ψ_{CAS} , without Constraints on the Overlaps between Active Orbitals^a

	$E_{CAS}/\text{hartree}$	$E_{VB}/\text{hartree}$	$W_1/\%$	$W_2/\%$	$W_3/\%$	$W_{VB}/\%$	S_{VB}	Δ_{12}	$P_k/\%$
B_6	-147.58646	-147.57957	0.26	0.80	0.03	98.91	0.994	0.524	40.1
C_6H_6	-230.78709	-230.77945	0.29	0.64	0.02	99.05	0.995	0.524	40.5
N_6	-326.55682	-326.54893	0.36	0.45	0.01	99.18	0.996	0.503	39.7
Al_6	-1451.14614	-1451.14161	0.31	1.08	0.06	98.56	0.993	0.483	38.0
Si_6H_6	-1736.92653	-1736.92173	0.33	0.85	0.04	98.78	0.994	0.481	38.5
P_6	-2044.34756	-2044.34329	0.37	0.55	0.02	99.06	0.995	0.453	37.9

^a See also eqs 1–4 and the definitions in the text. Δ_{12} is the nearest-neighbor orbital overlap and P_k is the Chirgwin–Coulson weight of a single Kekulé-like mode of spin coupling.

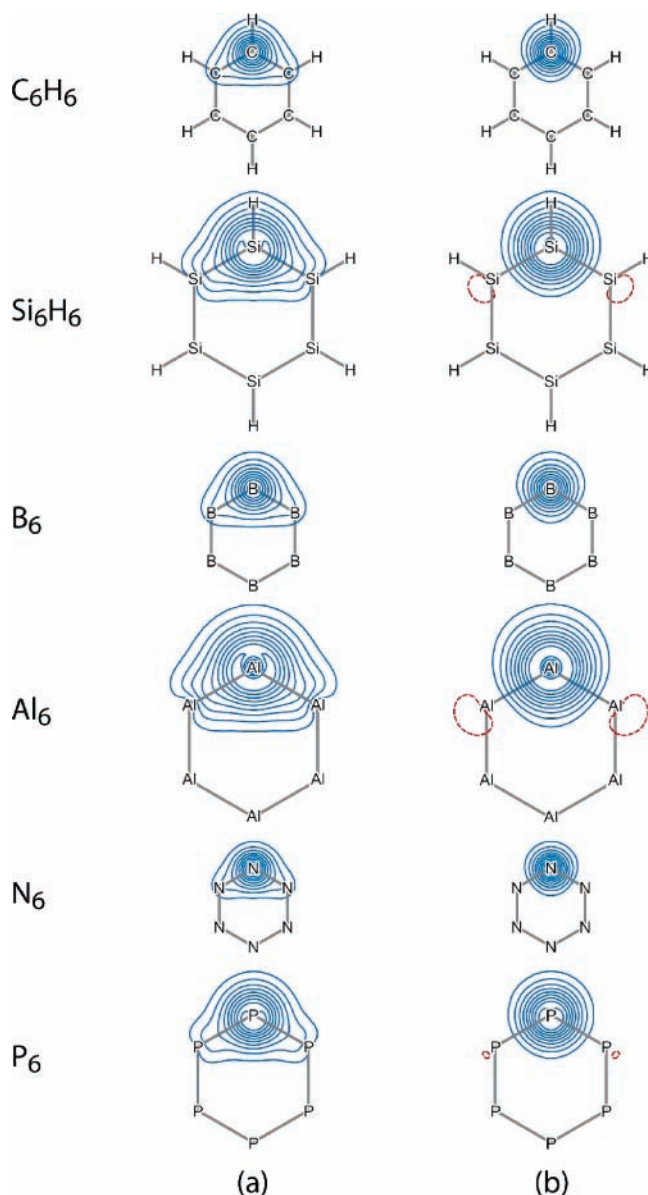


Figure 1. Contours in the plane 0.5 \AA above the molecular plane of symmetry unique active orbitals for various D_{6h} ring systems, generated by transforming the CASSCF wave function (a) without constraints on the overlaps between the active orbitals (left-hand column) and (b) with mutual orthogonality imposed (right-hand-column). Projected positions of the nuclei are shown by chemical symbols, together with the molecular framework. Contour heights were selected using the scheme described in the text.

of spin coupling (see Table 2), so that values of P_k are now on the order of 17–18%, with a higher net contribution from Dewar-like modes of spin coupling. It is also clear from Table 2 that the values of E_{VB} are somewhat discouraging. Indeed, the values of S_{VB} (not listed) are also very small indeed, so that

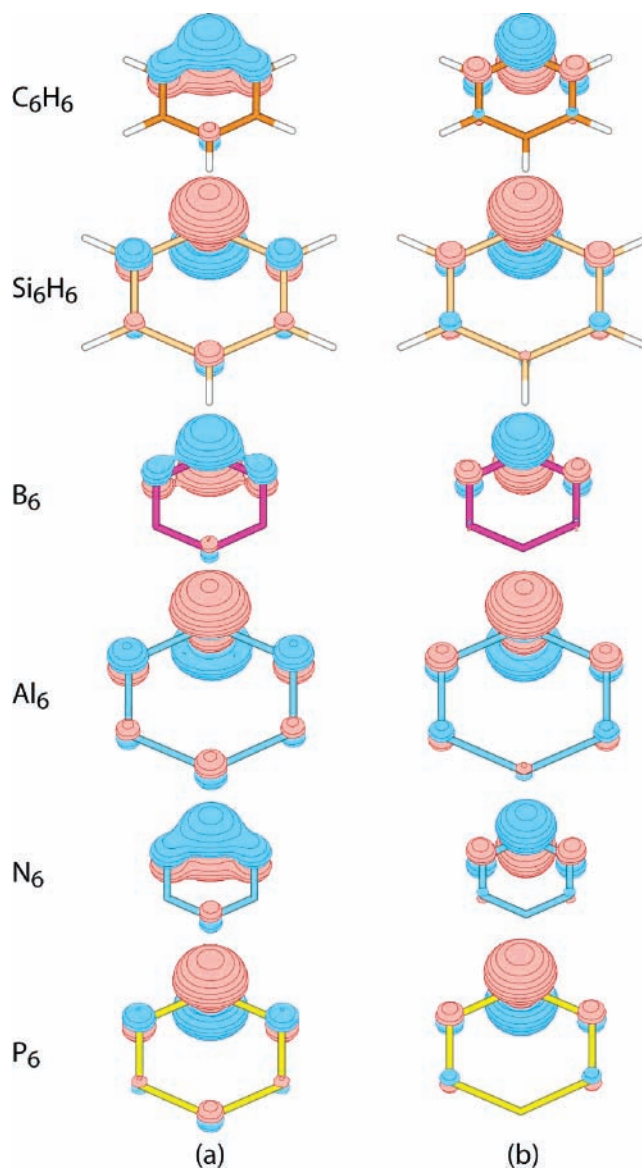


Figure 2. Symmetry unique active orbitals for various D_{6h} ring systems, generated by transforming the CASSCF wave function (a) without constraints on the overlaps between the active orbitals (left-hand column) and (b) with mutual orthogonality imposed (right-hand-column). Isovalues $\pm v$ were selected using the scheme described in the text. The orbitals are the same ones as those shown in Figure 1.

our analysis of the (large) orthogonal complement is somewhat less meaningful than before. As shown in Table 2, the largest contributions to Ψ_{VB} come from structures with one doubly occupied orbital (47–49%), with also significant values for W_2 (17–25%) and even nontrivial values of W_3 (exceeding 2% in B_6 and C_6H_6). For each of these ring systems, the values of W_{VB} are significantly lower than are those of W_1 . All in all, this particular representation of Ψ_{CAS} is rather disappointing.

TABLE 2: Key Quantities Obtained by Optimizing the Importance of Ψ_{VB} in Ψ_{CAS} , Subject to Orthogonality Constraints between All of the Active Orbitals^a

	$E_{VB}/\text{hartree}$	$W_1/\%$	$W_2/\%$	$W_3/\%$	$W_{VB}/\%$	$P_K/\%$
B ₆	-147.02918	49.03	25.36	2.37	23.24	17.1
C ₆ H ₆	-230.11572	49.16	24.41	2.20	24.23	17.3
N ₆	-325.86433	48.72	20.82	1.65	28.80	17.6
Al ₆	-1450.89579	48.21	22.21	1.92	27.65	17.0
Si ₆ H ₆	-1736.63380	48.15	21.01	1.74	29.10	17.3
P ₆	-2044.07052	46.57	16.64	1.18	35.61	17.5

^a The various symbols have the same meaning as in Table 1.

Before examining further these various sets of numerical values, it is instructive also to consider the outcome of fully variational optimization of wave functions (Ψ_{SC}) of the form shown in eq 1. The resulting total energies E_{SC} are listed in Table 3, together with various other quantities. As before, we obtained solutions with six symmetry equivalent, relatively localized nonorthogonal active orbitals ψ_μ . The shapes of these orbitals are practically indistinguishable by eye from the nonorthogonal set shown in the left-hand columns of Figures 1 and 2. The reoptimization of the inactive orbitals, and the freedom of the ψ_μ to incorporate (small) contributions from the CASSCF virtual space, leads only to a very modest lowering of E_{SC} over the corresponding value of E_{VB} (Table 1). Similarly, there are only very small changes in the nearest-neighbor orbital overlaps and the Chirgwin–Coulson weights of a single Kekulé-like mode of spin coupling, so that the fully variational wave function is very similar indeed to the very strongly dominant Ψ_{VB} component of Ψ_{CAS} , described earlier. To a very large extent, we may consider Ψ_{SC} and the (unconstrained) Ψ_{VB} to be almost interchangeable in our subsequent analysis.

It is entirely straightforward to evaluate the total energy corresponding to various subsets of the full spin space, without reoptimizing any of the inactive or active orbitals in Ψ_{SC} . We report in Table 3 the energies E_{1K} and E_{2K} for a single Kekulé-like mode of spin coupling and for both such modes, respectively. The relatively small values of $|E_{SC} - E_{2K}|$ provide further confirmation of the dominance of these Kekulé-like modes in the active-space spin coupling patterns. The differences $E_{RES} = |E_{SC} - E_{1K}|$ may be regarded as spin-coupled estimates of the resonance energy and it could be useful also to examine the proportion (Q_{RES}) that such values represent of the total active-space-only electronic energies. Values of E_{res} and Q_{res} are collected in Table 3. In our opinion, comparing Q_{res} values is more meaningful than comparing the actual resonance energies E_{res} , as the Q_{res} values are much less dependent on the environments “inhabited” by the active electrons in the different rings (consider the fact that the Hartree–Fock energies of the occupied π orbitals, e.g., in N₆, are lower than the energies of the corresponding orbitals in C₆H₆). It should be emphasized that neither of the other two quantities we use to analyze relative aromaticities, the nearest-neighbor orbital overlap Δ_{12} or the Chirgwin–Coulson weight of a single Kekulé-like mode of spin coupling P_K , is influenced appreciably by the “inactive” part of the molecule.

Examining various quantities from the descriptions without constraints on the overlaps between the active orbitals, we observe a fairly consistent ordering of the different ring systems according to their degree of aromaticity:

$$C_6H_6 \sim B_6 > N_6 > Al_6 \sim Si_6H_6 > P_6$$

Except for minor reordering of similar values, this is the case for Δ_{12} (nearest-neighbor orbital overlap), P_K (Chirgwin–Coulson weight of a single Kekulé-like mode of spin coupling)

and Q_{res} (resonance energy scaled by the active-space-only electronic energies). We observe that the basic pattern is much the same for the rings based on first-row or second-row atoms, but that values for the first-row rings are larger than are those for their second-row analogues. The differences between the aromaticities of rings constructed from atoms from the same row are much smaller than those corresponding to rings of atoms from different rows.

The representation based on orthogonal active orbitals is somewhat different. In the limit of strictly localized orbitals, as in classical VB, we could interpret structures with doubly occupied orbitals as “ionic”. With this in mind, we see from Table 2 that the ring systems that appeared to be most aromatic actually turn out to be the least covalent, in the sense of having the smallest values of W_{VB} . Indeed, the largest net contributions to Ψ_{CAS} are due to the singly ionic structures, with the largest values of W_1 corresponding to the largest values of Δ_{12} , P_K and Q_{res} in the nonorthogonal description. These W_1 values, which measure to a large extent the inability of a strictly orthogonal description to describe properly the orbital deformations (and so on) seen in the unconstrained representations, are ordered as

$$C_6H_6 \sim B_6 > N_6 > Al_6 \sim Si_6H_6 > P_6$$

This pattern does of course coincide with the one presented earlier and so, in principle, could be used as an alternative measure of the degree of aromaticity. Nonetheless, we consider this a somewhat perverse approach, given that these W_1 values measure to a large extent the inadequacy of the covalent-only orthogonal orbital description.

Sakai has suggested an alternative criterion for the aromaticity of these six-membered rings, using the differences between the weights of different contributions to a particular orthogonal orbital representation of the CASSCF wave functions.³ In essence, the CiLC (CI/LMO/CASSCF) method involves localizing the CASSCF active-space canonical orbitals using the Boys criterion, and then performing a CI calculation using the same configuration list as in the CASSCF.¹⁰ As in our own work, the outcome is an alternative representation of the full CASSCF wave function. The CI calculations in the CiLC study were performed at the determinantal level, so that the largest single contribution for each system comes from the “covalent” arrangement (with six singly occupied orbitals) with alternating one-electron spins (α , β) around the ring. Further covalent arrangements, but with adjacent pairs of α or β spins, were labeled “singlet coupling” terms. Similarly, singly ionic arrangements with adjacent charges (i.e., with one doubly occupied orbital neighboring an empty site), but otherwise alternating α and β spins around the ring, were labeled “polarization” terms. The relevant sums of squares of CI coefficients were taken as the overall weights of these so-called singlet coupling and polarization terms. The proposed new criterion in ref 3 relies directly on the difference between these two weights, with smaller differences or “gaps” supposedly indicating higher aromaticity. The resulting ordering appears to be as follows:

$$B_6 < C_6H_6 < Al_6 < N_6 \sim Si_6H_6 < P_6$$

(2.5) (10) (39) (49) (112)

where the numbers in brackets are our own estimates of the *relative* gaps, based on examining Figure 7 in that paper. For these six molecules, the gap increases rather rapidly both across a row and down a column of the periodic table, so that this quantity does not provide a linear measure of the degree of aromaticity. On closer examination of Sakai’s Figure 7,³ we

TABLE 3: Total Spin-Coupled Energies (E_{SC}) and Nearest-Neighbor Orbital Overlaps (Δ_{12}) from Fully variational Optimization^a

	$E_{SC}/\text{hartree}$	Δ_{12}	$P_K/\%$	$E_{1K}/\text{hartree}$	$E_{2K}/\text{hartree}$	$E_{res}/\text{mhartree}$	$Q_{res}/\%$
B_6	-147.57970	0.524	40.1	-147.55423	-147.57942	25.5	0.495
C_6H_6	-230.77955	0.524	40.4	-230.74770	-230.77921	31.8	0.494
N_6	-326.54898	0.503	39.7	-326.51048	-326.54839	38.5	0.457
Al_6	-1451.14172	0.484	38.1	-1451.12814	-1451.14145	13.6	0.389
Si_6H_6	-1736.92181	0.481	38.5	-1736.90525	-1736.92148	16.6	0.382
P_6	-2044.34332	0.453	37.9	-2044.32504	-2044.34282	18.3	0.352

^a Also listed are the values of E_{1K} , E_{2K} , E_{res} , and Q_{res} described in the text, and the Chirgwin–Coulson weights (P_K) of a single Kekulé-like mode of spin coupling.

notice that the variation in the singlet coupling weight is much more dramatic than that for the polarization weight, and so it accounts for much of the variation in the “gap” from one system to another. This is both a convenience, because it means that fewer coefficients need to be analyzed, and also a potential cause for concern. As in our own orthogonal orbital representation of each system, the total weight of all the covalent contributions must be relatively small. By concentrating on a subset of those contributions, with weights that are less than 0.021 for B_6 and that are still less than 0.032 for P_6 , this particular criterion of aromaticity seems to us to rely rather heavily on examining rather minor contributions to the total wave function. In this sense, at least, we prefer our own criteria that are based instead on quantities that are derived directly from a largely predominant component of the total wave function.

A magnetic criterion for the aromaticity of these systems is provided by the contributions from the π bonds to the total nucleus-independent chemical shift (NICS) values calculated for a point 0.5 Å above the ring center. The NICS(π) values reported by von Schleyer and co-workers¹¹ are C_6H_6 (-16.8), N_6 (-15.9), P_6 (-14.7) and Si_6H_6 (-14.1). All results discussed in the present paper lead to the conclusion that C_6H_6 is more aromatic than N_6 , and that the D_{6h} rings based on first-row atoms are more aromatic than their second-row analogues. On the other hand, our criteria as well as the one used by Sakai³ suggests that Si_6H_6 is more aromatic than P_6 , whereas the fairly close NICS(π) values suggest the opposite order.

The C_6H_6 , N_6 , P_6 and Si_6H_6 (constrained) D_{6h} rings have also recently been considered by Engelberts et al.¹² who used a combination of VB calculations based on strictly atomic nonorthogonal orbitals, fully variational spin-coupled calculations, and the analysis of current-density maps in a study of various “inorganic benzenes”. All four of these homonuclear systems showed characteristics of aromaticity, similar to those described here. Indeed, were it not for some differences in the basis sets and geometries, the fully variational spin-coupled results in their paper and in ours would coincide. They report that C_6H_6 and N_6 show strong ring currents, with those for the second row analogues being less than half the strength calculated for benzene.

Conclusions

Starting from CASSCF(6,6)/6-31G(d,p) wave functions, we have considered different interpretations of the π electron systems for various (constrained) “benzene-like” D_{6h} rings, exploiting the invariance of the total wave function to arbitrary nonsingular transformations of the active orbitals. Various quantities that are obtained rather directly from our various calculations provide a fairly consistent ordering of the degree of aromaticity in these different ring systems: $C_6H_6 \sim B_6 > N_6 > Al_6 \sim Si_6H_6 > P_6$.

It may of course be most convenient for many purposes to use canonical orbitals that transform as irreducible representa-

tions of the molecular point group. For others, it may be more instructive to examine representations of the CASSCF wave function that are based on relatively localized orbitals, perhaps resembling those envisaged in classical valence bond theory. Ultimately, though, none of these representations of precisely the same total wave function is any more “correct” than any other. On the other hand, if a representation based on orthogonal orbitals appears (at first sight) to give a conflicting assessment of the various VB-like characteristics of that wave function, then it could be useful to bear in mind that valence bond theory is of course traditionally based on notions of nonorthogonal localized orbitals. Our own particular preference, as illustrated here, is to consider representations in which a very compact VB-like component based on nonorthogonal relatively localized orbitals is overwhelmingly dominant. We also find, at least for the systems considered here, that subsequent variational optimization of such a VB-like description leads only to rather modest further changes.

References and Notes

- (1) Garratt, P. J. *Aromaticity*; Wiley: New York, 1986.
- (2) Hiberty, P. C.; Shaik, S. *Theor. Chem. Acc.* **2005**, *114*, 169.
- (3) Sakai, S. *J. Phys. Chem. A* **2002**, *106*, 10370.
- (4) Frisch, M. J.; Trucks, G. W.; Schlegel, H. B.; Scuseria, G. E.; Robb, M. A.; Cheeseman, J. R.; Zakrzewski, V. G.; Montgomery, J. A.; Stratmann, R. E.; Burant, J. C.; Dapprich, S.; Millam, J. M.; Daniels, A. D.; Kudin, K. N.; Strain, M. C.; Farkas, O.; Tomasi, J.; Barone, V.; Cossi, M.; Cammi, R.; Mennucci, B.; Pomelli, C.; Adamo, C.; Clifford, S.; Ochterski, J.; Petersson, G. A.; Ayala, P. Y.; Cui, Q.; Morokuma, K.; Malick, D. K.; Rabuck, A. D.; Raghavachari, K.; Foresman, J. B.; Cioslowski, J.; Ortiz, J. V.; Baboul, A. G.; Stefanov, B. B.; Liu, G.; Liashenko, A.; Piskorz, P.; Komaromi, I.; Gomperts, R.; Martin, R. L.; Fox, D. J.; Keith, T.; Al-Laham, M. A.; Peng, C. Y.; Nanayakkara, A.; Gonzalez, C.; Challacombe, M.; Gill, P. M. W.; Johnson, B.; Chen, W.; Wong, M. W.; Andres, J. L.; Head-Gordon, M.; Replogle, E. S.; Pople, J. A. *Gaussian 98* revision A.7; Gaussian: Pittsburgh, PA, 1998.
- (5) MOLPRO, a package of ab initio programs designed by H.-J. Werner and P. J. Knowles, version 2002.8, R. D. Amos, A. Bernhardsson, A. Berning, P. Celani, D. L. Cooper, M. J. O. Deegan, A. J. Dobbyn, F. Eckert, C. Hampel, G. Hetzer, P. J. Knowles, T. Korona, R. Lindh, A. W. Lloyd, S. J. McNicholas, F. R. Manby, W. Meyer, M. E. Mura, A. Nicklass, P. Palmieri, R. Pitzer, G. Rauhut, M. Schütz, U. Schumann, H. Stoll, A. J. Stone, R. Tarroni, T. Thorsteinsson, and H.-J. Werner.
- (6) (a) Cooper, D. L.; Gerratt, J.; Raimondi, M. *Chem. Rev.* **1991**, *91*, 929. (b) Gerratt, J.; Cooper, D. L.; Karadakov, P. B.; Raimondi, M. In *Handbook of Molecular Physics and Quantum Chemistry*; Wilson, S., Ed.; Wiley: Chichester, 2003; Vol. 2, Part 2, Chapter 12, pp 148–68.
- (7) (a) Thorsteinsson, T.; Cooper, D. L.; Gerratt, J.; Karadakov, P. B.; Raimondi, M. *Theor. Chim. Acta* **1996**, *93*, 343. (b) Cooper, D. L.; Thorsteinsson, T.; Gerratt, J. *Adv. Quantum Chem.* **1998**, *32*, 51. (c) Thorsteinsson, T.; Cooper, D. L. *J. Math. Chem.* **1998**, *23*, 105.
- (8) Chirgwin, B. H.; Coulson, C. A. *Proc. R. Soc. London, Ser. A* **1950**, *201*, 196.
- (9) Karadakov, P. B.; Gerratt, J.; Cooper, D. L.; Raimondi, M. *J. Chem. Phys.* **1992**, *97*, 7637.
- (10) Sakai, S. *J. Phys. Chem. A* **2000**, *104*, 922.
- (11) Schleyer, P. v. R.; Jiao, H.; van Eikema Hommes, N. J. R.; Malkin, V. G.; Malkina, O. L. *J. Am. Chem. Soc.* **1997**, *119*, 12669.
- (12) Engelberts J. J.; Havenith, R. W. A.; van Lenthe, J. H.; Jenneskens, L. W.; Fowler, P. W. *Inorg. Chem.* **2005**, *44*, 5266.